Prediction of Pest Occurrence Risk and Spatial Patterns Based on a Novel Synergistic Fusion BiLSTM approach

Xinyi Liu [1], Delong Kong [2], Xin Jiang [3], Xiaopeng Wang [4], Jiahua Zhang [5*]
[1-5] Remote Sensing Information and Digital Earth Center, School of Computer Science and Technology, Qingdao University, Qingdao 266071, China
[5] Key Laboratory of Digital Earth Science, Aerospace Information Research Institute, Chinese Academy of Sciences, Beijing 100094, China

* Corresponding Author: **Jiahua Zhang**

Article Info

P-ISSN: 3051-3383
E-ISSN: 3051-3391
Volume: 06
Issue: 02
July - December 2025
Received: 09-09-2025
Accepted: 11-10-2025
Published: 10-11-2025
Page No: 87-101

Abstract
The invasive pest Hyphantria cunea poses a serious threat to forestry and agricultural ecosystems. To mitigate this threat, accurate and efficient prediction of its distribution is critical for enabling proactive management and targeted control strategies. However, existing traditional statistical models and machine learning approaches exhibit limited predictive performance due to their inability to effectively capture complex spatiotemporal dependencies and process multi-source heterogeneous data. Furthermore, although deep learning has demonstrated progress in pest prediction, current models still suffer from critical limitations including inadequate feature fusion and insufficient critical temporal feature capture. To address this issue, this study proposes a novel Synergistic Fusion Bidirectional Long Short-Term Memory network (SF-BiLSTM). Centered on the synergistic fusion of multi-source heterogeneous data, its architecture consists of three core stages. Firstly, a Bidirectional LSTM (BiLSTM) is utilized to capture complex spatiotemporal dependencies within environmental sequences. Subsequently, dual-path temporal feature refinement is performed: one path employs mean pooling and layer normalization for feature compression, while the other integrates an attention sub-network to focus on critical time steps and conduct weighted fusion. Finally, an adaptive weighted fusion of the dual-path features is achieved through a weight learning network, yielding the final risk prediction. Experiments on the Shandong Province dataset from 2019 to 2024 demonstrate that the SF-BiLSTM model achieves outstanding comprehensive performance, with a Precision of 0.9667 and an F1-score of 0.9496, significantly outperforming traditional machine learning methods such as Gradient Boosting, KNN, and all baseline models. This model successfully reveals the spatiotemporal patterns and risk levels of Hyphantria cunea outbreaks in Shandong Province, providing reliable decision support for precise regional pest prevention and control.

DOI: https://doi.org/10.54660/IJAIET.2025.6.2.87-101

Keywords: Hyphantria Cunea, Spatio-Temporal Prediction, Bilstm, Multi-Source Heterogeneous Data, Pest Risk Prediction

1. Introduction

The Hyphantria cunea (Drury), a highly adaptive pest native to North America, has a broad host range and has invaded continents including Asia and Europe, posing a significant threat to global forestry, agriculture, and urban landscapes (Macfadyen S *et al* ,2012) [17]. In China's Shandong Province, this pest has inflicted severe damage on local poplar plantations, shelterbelts, and urban greenbelts in recent years. Its high fecundity and the extensive feeding habits of its larvae facilitate rapid colonization and spread, severely threatening ecological balance and economic development (Sourakov A *et al*,2010) [20].

The larval feeding behavior critically impairs plant health, potentially leading to tree mortality and causing substantial economic losses to biodiversity and related industries. Therefore, developing precise and efficient prediction techniques for Hyphantria cunea outbreaks is of significant theoretical and practical value for formulating early warning and targeted control strategies.

Early pest prediction methods primarily relied on traditional statistical models, such as ARIMA time-series analysis and multiple regression models (Kawakita S *et al*,2022) [17] to analyze historical dynamics or quantify the relationship between meteorological factors and pest development. While these models can analyze historical trends, they struggle to capture complex non-linear interactions and deep spatiotemporal dependencies. With advancements in computational science, machine learning algorithms like Support Vector Machines (SVM), Artificial Neural Networks (ANN), and KNN have been applied to pest risk prediction, improving accuracy due to their proficiency in handling complex non-linear relationships (Xiao Q *et al*,2019) [21]. However, these methods still face challenges, including sensitivity to data quality, and insufficient capability to effectively capture complex spatiotemporal dependencies and process multi-source heterogeneous data which limit their utility in managing complex pest systems.

In recent years, deep learning-based artificial intelligence has demonstrated revolutionary potential in the intelligent monitoring and prediction of agricultural pests, owing to its end-to-end learning, automatic feature extraction, and complex pattern modeling capabilities (Kamilaris A *et al*,2019) [14]. Recurrent Neural Networks (RNN) and their variants, Long Short-Term Memory (LSTM) and Gated Recurrent Units (GRU), have been successfully applied to various crop pest predictions by effectively learning long-term dependencies while mitigating gradient-related problems (Xiao Q *et al*,2019) [17]. The Bidirectional Long Short-Term Memory (BiLSTM) network further enhances the ability to capture temporal dependencies by integrating both forward and backward information, achieving a more comprehensive understanding of each time step and outperforming unidirectional LSTM (Chen P *et al*,2020) [17]. Despite significant progress in deep learning, existing models for predicting complex invasive pests like Hyphantria cunea still face bottlenecks in multi-source heterogeneous data fusion, critical temporal feature capture, thereby limiting improvements in prediction accuracy, robustness, and practical applicability.

To address the limitations of existing prediction methods for the Hyphantria cunea, this study aims to develop an intelligent prediction model for H. outbreak trends with significant enhancements in prediction accuracy and model robustness. To address limitations of existing Hyphantria cunea prediction methods, this study proposes the novel SF-BiLSTM. It uses BiLSTM to capture spatiotemporal dependencies, optimizes temporal features via dual paths, and achieves adaptive fusion through a weight learning network for final risk prediction, thereby improving accuracy and robustness to support smart agriculture.

2. Related Work

Research on pest and disease forecasting has undergone a paradigm shift from experience-dependent to data-driven approaches. Early studies were primarily based on empirical knowledge and expert judgment, with statistical models serving as the main analytical tools. For instance, degree-day models based on heat accumulation have been widely used for predicting pest developmental stages (Ebbenga DN *et al*,2022) [17]. With the introduction of time series analysis techniques, models such as ARIMA have provided new methods for forecasting pest and disease occurrence trends (Kawakita S *et al*,2022) [17], while regression models have sought to establish quantitative relationships between meteorological factors and pest incidence [17]. These traditional methods have laid an important foundation for pest and disease prediction, but their limitations in handling nonlinear relationships and complex environmental interactions have prompted researchers to turn to more advanced machine learning approaches.

The advent of Machine Learning (ML) provided more sophisticated tools for pest forecasting. Algorithms such as Support Vector Machines (SVM) and Random Forests (RF) have been widely adopted. SVM, for example, has been used for risk level classification (Pedregosa F *et al*,2011) [19] while RF has demonstrated robust performance in handling high-dimensional data and ranking feature importance for prediction (Ding W *et al*,2016) [17]. These methods offered improvements over traditional models by processing multi-source data and identifying non-obvious correlations.

Deep Learning (DL) models have further revolutionized the field through their capacity for automatic learning of hierarchical feature representations. Although this study focuses on time series, Convolutional Neural Networks (CNNs) are relevant in smart agriculture, particularly for their outstanding performance in image-based crop disease identification and remote sensing data analysis (Huang Y *et al*,2024) [17]. Given the temporal nature of pest development and environmental influences, Recurrent Neural Networks (RNNs) and their variants, especially Long Short-Term Memory (LSTM) networks and Gated Recurrent Units (GRU), have become central to modern pest forecasting. LSTM is capable of capturing long-term dependencies (Gao Z *et al*,2023) [17] and has been successfully applied to predict pest population dynamics, disease incidence rates, and risk levels (Hang J *et al*,2019) [17]. GRU, with its simpler architecture, has also shown comparable performance in similar tasks (Cho K *et al*,2014) [17]. To leverage contextual information within sequences, Bidirectional LSTM (BiLSTM) has been employed; it processes input sequences in both directions to gain a more comprehensive understanding of temporal patterns and has outperformed unidirectional LSTM in various time-series forecasting tasks, including pest prediction (Chen P *et al*,2020) [17].

The Attention Mechanism allows a model to dynamically weigh the importance of different parts of an input sequence during prediction, which is particularly beneficial for long sequences where information is not equally relevant (Pedregosa Fet al,2011) [19]. In pest forecasting, an attention mechanism can help a BiLSTM model focus on critical historical weather patterns or specific time lags, and its integration with LSTM has demonstrated improved performance. Ensuring that the risk probabilities output by pest prediction models are well-calibrated is essential for effective resource allocation and timely intervention. For multi-source feature fusion, traditional methods like Mixture of Experts (MoE) achieve heterogeneous data fusion through parallel learning of multiple subnetworks but suffer from high architectural complexity. In contrast, SF-BiLSTM innovatively designs a dual-path normalization + weight

learning network: one path uses Mean Pooling for feature compression, and the other path uses attention weighting to

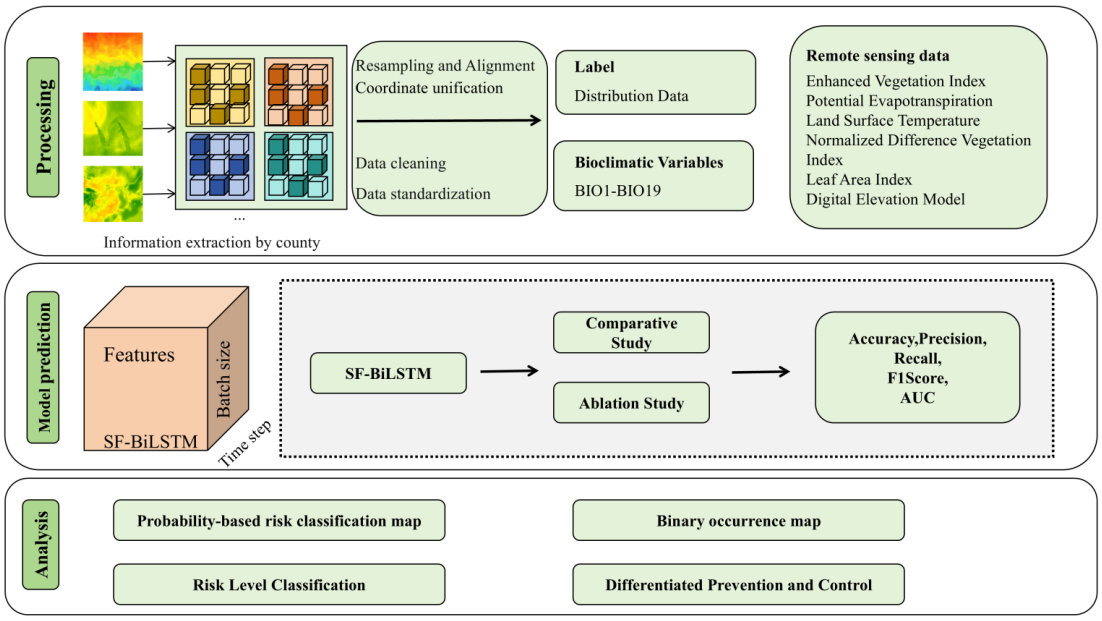

Fig 1: Workflow of proposed SF-BiLSTM.

emphasize key information. Finally, a Weight Learning Network adaptively assigns fusion weights. This design not only simplifies the fusion process of multi-source heterogeneous data (environmental + geographical) but also ensures the flexibility of feature fusion, representing a lightweight optimization of existing fusion mechanisms. Additionally, Layer Normalization has been proven to improve the training stability of deep models. SF-BiLSTM introduces this operation after both paths, further ensuring the distribution consistency of features before fusion and laying a foundation for subsequent weight learning and risk prediction.

3. Study Area and Data

The research workflow consists of three main core stages: preprocessing, model prediction, and result analysis as illustrated in Fig. 1. First, a comprehensive dataset established through a multi-step data preparation and preprocessing pipeline. The process began with the acquisition of raw data, including meteorological records, geographical information, and historical pest occurrences from the sources listed in Table 1. Second, predictions are made using the SF-BiLSTM model as shown in Fig. 3. SF-BiLSTM achieves high-precision and robust prediction of the occurrence risk of Hyphantria cunea through Synergistic fusion of multi-source heterogeneous data. Finally, based on model evaluation metrics, the results are analyzed to verify the advantages of the SF-BiLSTM.

To ensure spatial consistency, all geospatial data were first reprojected into a unified coordinate system and resampled to a uniform resolution. Subsequently, these multi-source data were precisely aligned in both the temporal and spatial dimensions to facilitate integrated analysis.

In the Model prediction stage, the proposed SF-BiLSTM model was trained, and its performance was rigorously evaluated via Comparative Study and Ablation Study. To ensure a fair comparison, all models were trained, validated, and tested on the same dataset partitions. Performance was assessed across a comprehensive suite of evaluation metrics, including Accuracy, Precision, Recall, F1Score, and AUC.

The Analysis stage involves analyzing the model outputs to reveal county-level risk patterns and demonstrate the practical value of the model. Specifically, it conducts analysis on the Probability-based risk classification map and performs Risk Level Classification, meanwhile analyzing the Binary occurrence map and developing Differentiated Prevention and Control strategies. By integrating these analysis results, it provides targeted decision support for precise prevention and control at the county scale.

To validate the contribution of each key component within our novel architecture, a series of ablation studies were conducted. We systematically removed or modified critical modules of the SF-BiLSTM, each variant was then trained and evaluated independently under the same conditions to precisely quantify the impact of each component on the overall model performance.

The final stage of the research workflow focuses on county-level analysis and interpretation of the model outputs. First, conduct in-depth analysis of the county-level predicted probability distributions and binary occurrence results to clarify the overall risk pattern at the county scale. Then, visualize this county-level prediction information on the geographical map of the study area to intuitively display the risk differences and occurrence statuses of each county. Finally, integrate and generate county-level Hyphantria cunea risk maps, providing actionable scientific basis and decision support for formulating precise prevention and control strategies at the county scale.

3.1. Study Area

Shandong Province is located on the eastern coast of China and in the lower reaches of the Yellow River, situated between 34°22.9′ and 38°24.01′ N latitude and 114°47.5′ and 122°42.3′ E longitude. The topography is characterized by a high central massif, grading into gentle slopes in the east, while the western and northern regions are low-lying and part of the Yellow River Alluvial Plain. The Shandong Peninsula extends between the Yellow Sea and the Bohai Sea, featuring

a long coastline. Major mountain ranges include Mount Tai and Mount Lao.

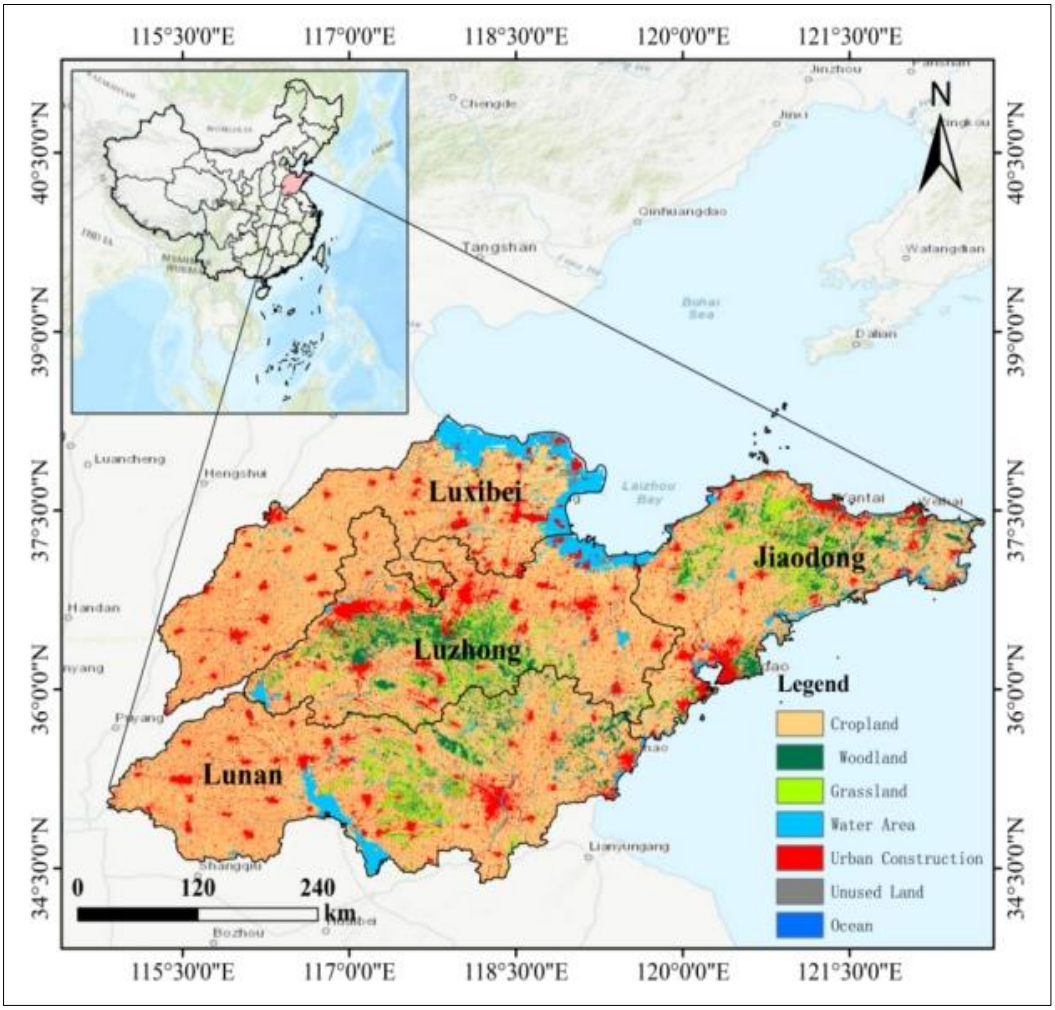

Fig 2: The study area of Shandong Province, China.

The province is in a temperate monsoon climate zone with four distinct seasons. Summers are hot and rainy, while winters are cold and dry. The average annual temperature ranges from 11°C to 14°C, and the average annual precipitation is between 550 mm and 950 mm. These climatic conditions provide a suitable environment for the growth and reproduction of numerous organisms, which also facilitates the survival and spread of invasive species such as Hyphantria cunea. As an international quarantine pest in forestry, Hyphantria cunea has caused severe damage to the forestry and urban greening of Shandong Province. In recent years, Shandong has been one of the key regions for the outbreak and control of Hyphantria cunea. A detailed map of the study area in Shandong is shown in Fig.2.

The spatial division of Shandong Province adopted in this study is established upon an ecological framework based on its inherent geographical patterns and climatic differentiation. The topography and climate of Shandong Province exhibit a significant west-to-east gradient, a pattern that directly determines the spatial heterogeneity in the potential distribution of the Hyphantria cunea. The vast Yellow River Alluvial Plain in the west and north features low-lying, flat terrain and distinct continental climate characteristics. Its high temperature stability and relatively mild winters provide excellent ecological conditions for the survival and spread of the Hyphantria cunea, constituting the theoretical core high-risk zone. Transitioning to the central and southern parts, the landforms of the Central-South Shandong Hills become undulating. This area serves as an ecological transition zone connecting the western plains and the eastern peninsula, with environmental conditions intermediate between the two. While harboring the potential for pest establishment, it is also constrained by topography, thus making it a crucial corridor for pest dispersal and a moderate-risk zone. Reaching the eastern Jiaodong Peninsula, the pronounced moderating influence of the maritime climate results in temperature and humidity combinations that deviate from the optimal survival conditions for the Hyphantria cunea, thereby forming a natural environmental barrier that suppresses population establishment and rendering it a low-risk suppression zone in model predictions. Consequently, the regional division in this study profoundly reveals the environmentally driven pattern of pest risk, laying a scientific foundation for subsequent precise monitoring and zonal management.

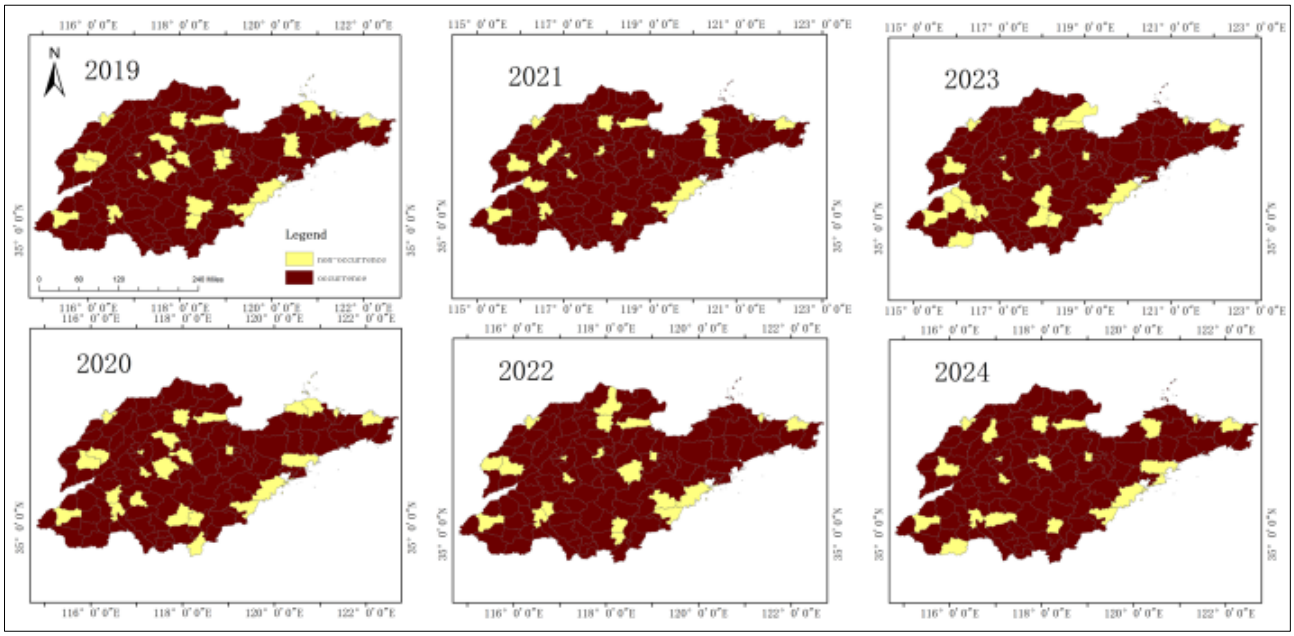

Fig 3: The actual distribution of Hyphantria cunea

3.2. Data sources and processing

3.2.1. Hyphantria cunea distribution data

Hyphantria cunea is widely distributed in Shandong Province. The distribution data of Hyphantria cunea in this paper were obtained from the National Forestry and Grassland Administration and the National Park Administration (https://www.forestry.gov.cn/), and the grade data were from the Shandong Provincial Department of Natural Resources (http://dnr.shandong.gov.cn/). The occurrence of Hyphantria cunea from 2019 to 2024 was collated as real data, covering 137 county - level administrative regions in Shandong. The occurrence in year, city, and county was recorded, and the county - level administrative unit was taken as the smallest analysis unit, with a total of 810 records.

The actual distribution data of Hyphantria cunea is shown in Fig. 3. It accounts for about 87% of the entire province, covering 119 out of 137 counties, and is mainly concentrated in the southwest Shandong Plain (Heze, Jining), northwest Shandong (Liaocheng, Dezhou) and the edge of the southern Shandong Hills (Linyi, Zaozhuang). The non - occurrence areas are sporadically distributed in the central Shandong mountainous area (Lixia District of Jinan, Taishan District of Tai'an), parts of the Jiaodong Peninsula (early stage in Rushan City of Weihai) and some counties in the Yellow River Delta (Dongying District of Dongying), accounting for about 13%.

3.2.2. Environmental Variables

Nineteen bioclimatic variables (e.g., Annual Mean Temperature, Minimum Temperature of Coldest Month, Annual Precipitation, Precipitation of Driest Quarter) were acquired from the WorldClim database (Version 2.1) (Fick SE *et al*,2017) [17], refer to Table 1 for details. These variables reflect the temperature and precipitation conditions and their seasonal variations within the study area, which significantly influence the growth, development, and reproduction of the Hyphantria cunea.

Considering the impact of vegetation status and land surface conditions on the pest's distribution, this study also incorporated the following remote sensing data: NDVI (Normalized Difference Vegetation Index): Reflects vegetation health and coverage. EVI (Enhanced Vegetation Index) [17]: Exhibits higher sensitivity in areas with dense vegetation, providing a better reflection of vegetation structure and canopy information. LST (Land Surface Temperature): Directly affects the metabolic rate and activity of insects. PET (Potential Evapotranspiration): Indicates the regional water deficit. LAI (Leaf Area Index): Represents the ratio of the total leaf area of the vegetation canopy to the ground surface area, which is correlated with the abundance of host plants. Finally, topographical data from a Digital Elevation Model (DEM) were also included.

Table 1: Environmental Variables Input Data

Variable	Name
BIO1	Annual Mean Temperature
BIO2	Mean Diurnal Range
BIO3	Isothermality
BIO4	Temperature Seasonality
BIO5	Max Temperature of Warmest Month
BIO6	Min Temperature of Coldest Month
BIO7	Temperature Annual Range
BIO8	Mean Temperature of Wettest Quarter
BIO9	Mean Temperature of Driest Quarter
BIO10	Mean Temperature of Warmest Quarter
BIO11	Mean Temperature of Coldest Quarter
BIO12	Annual Precipitation
BIO13	Precipitation of Wettest Month
BIO14	Precipitation of Driest Month
BIO15	Precipitation Seasonality
BIO16	Precipitation of Wettest Quarter
BIO17	Precipitation of Driest Quarter
BIO18	Precipitation of Warmest Quarter
BIO19	Precipitation of Coldest Quarter
EVI	Enhanced Vegetation Index
PET	Potential Evapotranspiration
LST	Land Surface Temperature
NDVI	Normalized Difference Vegetation Index
LAI	Leaf Area Index
DEM	Digital Elevation Model
Label	Hyphantria cunea Distribution Data

3.2.3. Data Preprocessing

This study implemented a systematic data preprocessing pipeline to handle multi-source heterogeneous data, ensuring data quality and consistency in model inputs. The process commenced with spatial reference unification, where all geospatial data were reprojected to the WGS84 coordinate system and resampled to a 1-kilometer spatial resolution using bilinear interpolation. This critical step effectively eliminated spatial discrepancies arising from differences in coordinate systems and scales, establishing a solid foundation for subsequent analyses.

In terms of sample construction, this study innovatively employed a buffer-constrained random sampling strategy to generate negative samples based on the geographical locations of Hyphantria cunea occurrence points. Specifically, spatial buffers with a 5-kilometer radius were established around known occurrence points, and an equivalent number of pseudo-absence points were systematically generated outside these areas. This approach not only effectively mitigated potential interference from spatial autocorrelation in model training but also ensured the ecological rationality of the sample set, providing balanced training data for the model.

Addressing the issue of missing values in environmental variables, this study designed a comprehensive missing value handling protocol. Initially, environmental variables with missing rates exceeding 80% were identified and eliminated to avoid the impact of low-quality data on model performance. Subsequently, a year-grouped median imputation method was applied to fill the remaining missing values while maintaining consistency in time-series characteristics. Through systematic quality verification, the final dataset was guaranteed to contain no remaining missing values, providing strong assurance for the stability of model training. All continuous environmental variables underwent Z-score standardization to effectively eliminate the influences of dimensional differences among variables.

The preprocessed dataset containing 810 samples was partitioned into training (70%, n=567), validation (20%, n=162), and test sets (10%, n=81) using stratified random sampling to maintain consistent class distribution across splits. This partitioning strategy ensures that the model is trained on a substantial portion of the data while reserving independent validation and test sets for hyperparameter tuning and unbiased performance evaluation, respectively.

3.2.4. Geographical Feature Encoding

To achieve effective integration of spatial contextual information with deep learning models, this study designed a specialized geographical feature encoding scheme. Utilizing the LabelEncoder component from the Scikit-learn machine learning library, textual county-level administrative division names were converted into unique integer identification codes. This conversion process strictly adhered to the principle of category order preservation, achieving data medicalization while completely maintaining the inherent discrete characteristics of geographical units.

The generated geographical feature vector through encoding serves as an independent feature channel, constituting a dual-path input architecture for the model together with environmental variable sequences. This design enables the model to fully identify spatial correlations and regional differences among different counties, providing rich spatial contextual information for the subsequent weighted fusion layer. The encoded geographical features dynamically interact with spatiotemporal features during model training, significantly enhancing the model's capability to capture region-specific ecological patterns and improving prediction accuracy and robustness.

4. Methodology

The core of our methodology is the Synergistic Fusion BiLSTM (SF-BiLSTM) model, a novel architecture designed for precise spatio-temporal prediction of pest occurrence risk. Asillustrated in Fig. 4, the model synergistically integrates temporal dynamics from environmental sequences with static spatial context from geographical features through a dedicated fusion pathway.

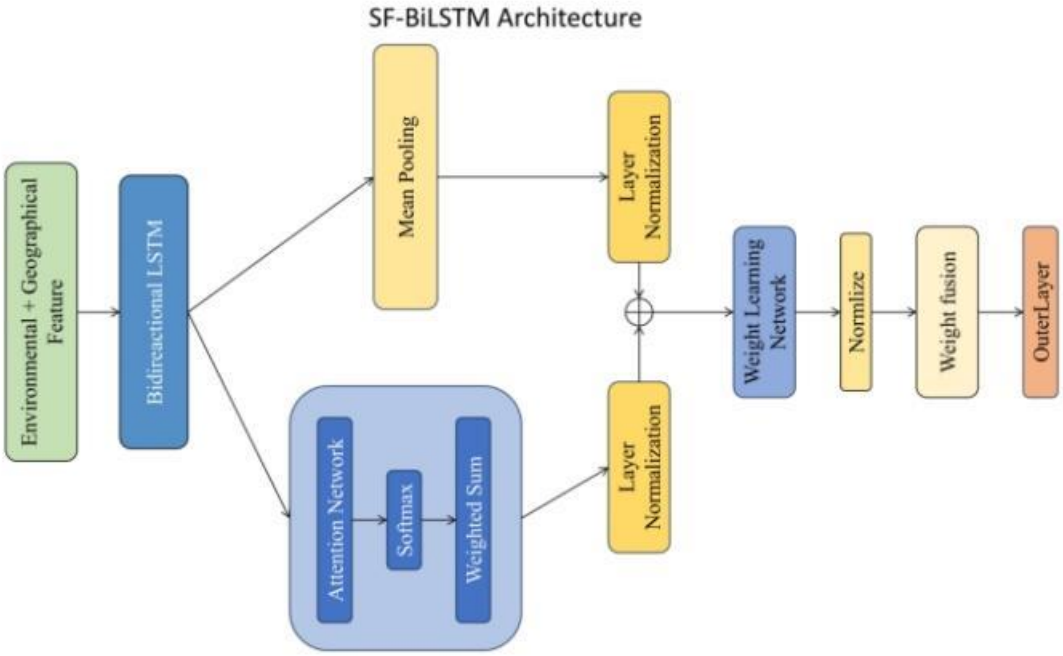

Fig 4: The architecture of the SF-BiLSTM model.

4.1. SF-BiLSTM Model Architecture

The Synergistic Fusion Bidirectional Long Short-Term Memory (SF-BiLSTM) model represents a novel deep learning architecture specifically designed for high-precision spatiotemporal prediction of pest occurrence risk. As illustrated in Figure 4, the model architecture comprises three interconnected stages: bidirectional spatiotemporal encoding, dual-path temporal feature refinement, and adaptive weighted fusion. This synergistic design enables effective integration of multi-source heterogeneous environmental data while capturing both critical and global temporal patterns essential for accurate pest outbreak prediction.

4.2. Bidirectional Spatiotemporal Encoding

The foundation of SF-BiLSTM lies in its bidirectional temporal modeling capability. The input layer receives preprocessed environmental time series with dimensions $X \in R^{(B*T*d_{in})}$, where Bdenotes batch size, T represents sequence length, and d_{in}= 25 encompasses environmental variables including 19 bioclimatic indicators (BIO1-BIO19), vegetation indices (NDVI, EVI), land surface characteristics (LST, LAI), water balance parameters (PET), and topographic information (DEM). In our dataset, each sample corresponds to a sequence of environmental conditions observed in a county across a given period.

These multi-dimensional time series are processed by a Bidirectional LSTM network, which simultaneously captures temporal dependencies in both forward and backward directions. Unlike traditional unidirectional LSTM that only considers past context, BiLSTM leverages information from both preceding and succeeding time steps, enabling comprehensive understanding of temporal patterns at each moment.

The BiLSTM achieves this by processing the input sequence in two separate directions, with the forward pass analyzing the sequence from start to end, and the backward pass analyzing it from end to start. The outputs from both directions are then combined at each time step. For each time step t∈ {1, 2, ..., T}, the forward LSTM computes:

$$f_t = \sigma\,(W_f \cdot [\overrightarrow{h_{t-1}}, x_t] + b_f) \quad (1)$$

$$i_t = \sigma\,(W_i \cdot [\overrightarrow{h_{t-1}}, x_t] + b_i) \quad (2)$$

$$\widetilde{C}_t = \tanh\,(W_C \cdot [\overrightarrow{h_{t-1}}, x_t] + b_C) \quad (3)$$

$$C_t = f_t \odot C_{t-1} + i_t \odot \widetilde{C}_t \quad (4)$$

$$o_t = \sigma\,(W_o \cdot [\overrightarrow{h_{t-1}}, x_t] + b_o) \quad (5)$$

$$\overrightarrow{h_t} = O_t \odot \tanh\,(C_t) \quad (6)$$

where $\sigma(\cdot)$ denotes the sigmoid activation function, $\tanh(\cdot)$ is the hyperbolic tangent activation, $\odot$ represents element-wise multiplication, $W_f, W_i, W_c, W_o \in R^{(d_h \times (d_h + d_{in}))}$ are weight matrices for forget, input, candidate, and output gates respectively, $b_f, b_i . b_o \in R^{d_h}$ are bias vectors, and d_h is the hidden dimension.

Symmetrically, the backward LSTM processes the sequence in reverse order (from T to1), computing backward hidden states $\overleftarrow{h_t}$ using identical gating mechanisms:

$$\overrightarrow{h_t} = \text{ForwardLSTM}(x_t, h_{t-1}) \quad (7)$$

$$\overleftarrow{h_t} = \text{BackwardLSTM}(x_t, \overleftarrow{h_{t+1}}) \quad (8)$$

The final representation at each time step concatenates forward and backward hidden states: By merging the outputs from both directions, the model generates a comprehensive contextual representation that captures the full temporal environment of each data point.

$$h_t = [\overrightarrow{h_t}, \overleftarrow{h_t}] \quad (9)$$

resulting in a BiLSTM output tensor $H \in R^{B \times T \times 2d_h}$.This bidirectional architecture is particularly crucial for pest prediction, as pest occurrence at any given time is influenced by both historical environmental accumulation (e.g., overwintering conditions, early-season temperature) and subsequent developmental conditions (e.g., breeding season climate, host plant phenology). The BiLSTM effectively captures these complex forward and backward causal relationships inherent in pest population dynamics.

4.3. Dual-Path Temporal Feature Refinement

Recognizing that different temporal scales and patterns contribute differently to pest occurrence prediction, SF-BiLSTM implements a parallel dual-path processing strategy to extract complementary temporal features from the BiLSTM output.

Attention-Based Critical Feature Extraction is the focus of this path. In the first pathway, we implement an attention mechanism designed to dynamically weight the most informative time steps. The core of this mechanism is a small, trainable network that executes these steps:

Specifically, this sub-network begins by mapping the hidden state at each time step to an attention score, which evaluates its relative importance. For each time step t, an intermediate representation is computed:

$$e_t = \tanh\,(W_1 \cdot h_t + b_1) \quad (10)$$

where $W_1 \in R^{d_h \times 2d_h}$ is a learnable weight matrix that projects the BiLSTM hidden state into the attention space, and$b_1 \in R^{d_h}$ is the bias vector.

This projection transforms the hidden states into a new space suitable for importance evaluation. These raw scores are then normalized to create a valid probability distribution. The intermediate representations are transformed into scalar attention scores and normalized:

$$\alpha_t = \frac{\exp\,(w_2^T e_t + b_2)}{\sum_{\tau=1}^{T} \exp\,(w_2^T e_\tau + b_2)} \quad (11)$$

where $W_2 \in \mathbb{R}^{d_h}$ is a learnable weight vector that maps the attention space to scalar scores, $b_2 \in R$ is a scalar bias, and

the softmax operation ensures that $\sum_t \alpha_t = 1$. The attention weights $\{\alpha_1, \alpha_2, \ldots, \alpha_T\}$ indicate the relative importance of each time step. The BiLSTM hidden states are aggregated using learned attention weights:

$$h_{attn} = \sum_{t=1}^{T} \alpha_t \odot h_t \in R^{2d_h} \quad (12)$$

This operation produces a fixed-size context vector through weighted summation, emphasizing key patterns. Subsequently, layer normalization is applied to this vector to standardize its values and ease the fusion process:

$$h_{attn}^{norm} = LayerNorm(h_{attn}) = \frac{h_{attn} - \mu}{\sqrt{\sigma^2 + \epsilon}} \odot \gamma + \beta \quad (13)$$

where μ and σ^2 are the mean and variance computed across the feature dimension, $\varepsilon = 1 \times 10^{-5}$prevents division by zero, and γ, $\beta = \in R^{2d_h}$ are learnable scale and shift parameters.This attention-based pathway excels at capturing critical phenological periods that disproportionately influence pest occurrence, such as overwintering survival rates determined by minimum winter temperatures, or peak larval development periods during spring warming. By learning which temporal windows are most predictive, the attention mechanism provides interpretable insights into the temporal drivers of pest outbreaks while focusing the model's capacity on the most informative signals.

To capture the general characteristics of the entire sequence, the second pathway employs temporal mean pooling. This method computes a simple average across all time steps, establishing a consistent baseline representation of global trends:

$$h_{pool} = \frac{1}{T} \sum_{t=1}^{T} h_t \in R^{2d_h} \quad (14)$$

Unlike attention-based selection, this approach provides a stable, comprehensive summary of environmental conditions throughout the entire observation period. Mean pooling effectively compresses temporal information into a fixed-length global representation, capturing baseline environmental characteristics while being robust to outliers and local fluctuations.

The pooled features from this pathway are then processed. To maintain consistency with the attention path and ensure stable feature scales for fusion, they are subjected to the same layer normalization operation.

$$h_{pool}^{norm} = LayerNorm(h_{pool}) \quad (15)$$

The complementary design of the two pathways is key to the model's effectiveness and robustness. While attention focuses on critical moments, mean pooling ensures that no important temporal information is completely discarded, providing a stable baseline representation. Both pathway outputs h_{pool}^{norm} and $h_{pool}^{norm} = \in R^{2d_h}$ are normalized to ensure consistent feature distributions before fusion.

4.4. Adaptive Weighted Fusion and Risk Prediction

The core innovation of SF-BiLSTM lies in its adaptive weighted fusion mechanism, which dynamically integrates the dual-path features based on their relevance to each specific prediction task. Rather than using fixed fusion strategies such as simple concatenation or uniform averaging, our model learns optimal fusion weights through a dedicated Weight Learning Network.

The normalized outputs from the attention and pooling paths are concatenated to form a unified representation that combines focused local patterns with global contextual information:

$$h_{combined} = [h_{attn}^{norm}; h_{pool}^{norm}] \in R^{4d_h} \quad (16)$$

This high-dimensional vector is then projected into a new representation space via a linear transformation. To enhance model robustness, a ReLU activation function is applied, and dropout is utilized during training to prevent overfitting.

$$z = Dropout(ReLU(W_{fci} h_{combined} + b_{fci})) \quad (17)$$

where $W_{fc1} \in R^{d_h \times 4d_h}$, $b_{fc1} \in R^{d_h}$, and the dropout rate is set to 0.3 for regularization.

This step involves the projection of the intermediate representation into a two-dimensional weight vector:

$$w_{raw} = Sigmoid(W_{fc2} z_1 + b_{fc2}) \quad (18)$$

where $W_{fc2} \in R^{2 \times d_h}$, $b_{fc2} \in R$, and the sigmoid activation constrains weights to [0, 1]. The output $w_{raw} = [w_{attn}^{raw}, w_{pool}^{raw}]^T \in R^2$ contains raw unnormalized weights for the two pathways.

We normalize the fusion weights so that they add up to 1:

$$w_{attn} = \frac{w_{attn}^{raw}}{w_{attn}^{raw} + w_{pool}^{raw} + \epsilon}, \; w_{pool} = \frac{w_{pool}^{raw}}{w_{attn}^{raw} + w_{pool}^{raw} + \epsilon} \quad (19)$$

The final fused representation is produced by a weighted summation of the two pathways' outputs, combining the focused attention with the global context into a unified representation.

$$h_{fused} = w_{attn} \cdot h_{attn}^{norm} + w_{pool} \cdot h_{pool}^{norm} \in R^{2d_h} \quad (20)$$

This weight learning mechanism enables the model to adaptively adjust feature contributions based on input characteristics. For instance, samples with pronounced seasonal patterns may receive higher attention pathway weights ($w_{attn} \approx 0.7 - 0.8$), while samples from environmentally stable regions may rely more on global pooled features ($w_{pool} \approx 0.6 - 0.7$). The adaptive nature of this fusion is key to the model's robustness across diverse environmental conditions.

The fused features h_{fuse} are transformed through a two-layer fully connected network for binary classification:

The first layer projects the high-dimensional input into a more compact representation. This dimensionality reduction is achieved through a linear transformation followed by ReLU

activation for nonlinearity, with dropout applied to enhance robustness.

$$z_{out}=\text{Dropout}(\text{ReLU}(W_{out1}h_{fused}+b_{out1})) \quad (21)$$

where $W_{out1}\in R^{d_h\times 2d_h}$, $b_{out1}\in R^{d_h}$, and dropout rate is 0.15 (half of the standard 0.3 rate for stability in the output stage). The network culminates in a final linear projection that condenses all learned features into a single scalar, representing the raw classification score.

$$\hat{y}=w_{out2}^{T}z_{out}+b_{out2}\in R \quad (22)$$

where $w_{out2}\in R^{d_h}$, $b_{out2}\in R$, the logit is processed by the sigmoid activation function, producing a continuous value that represents the event's probability of occurrence.

$$p(\text{occurrence})=\sigma(\hat{y})=\frac{1}{1+\exp(-\hat{y})}\in[0,1] \quad (23)$$

Table 2: Evaluation index

Metric	Definition	Formula
Accuracy	Proportion of correctly predicted samples among all samples	$\text{Accuracy}=\frac{TP+TN}{TP+TN+FP+FN}$
Precision	Proportion of true positives among samples predicted as positive	$\text{Precision}=\frac{TP}{TP+FP}$
Recall	Proportion of true positives correctly identified among all actual positives	$\text{Recall}=\frac{TP}{TP+FN}$
F1-Score	Harmonic mean of precision and recall	$\text{F1-Score}=2\times\frac{\text{Precision}\times\text{Recall}}{\text{Precision}+\text{Recall}}$
AUC-ROC	Area Under the Receiver Operating Characteristic curve (ability to distinguish classes)	$\text{AUC}=\frac{\sum_{i=1}^{m}\sum_{j=1}^{n}\left[\mathcal{I}(P_i^{+}>P_j^{-})+\frac{1}{2}\mathcal{I}(P_i^{+}=P_j^{-})\right]}{m\times n}$

Table 3: Comparative Experiments Results

Model	Accuracy	Precision	Recall	F1-Score	AUC
SF-BiLSTM	0.9136	0.9667	0.9851	0.9496	0.8657
Gradient Boosting	0.9006	0.9565	0.9451	0.9206	0.8264
KNN	0.9012	0.8933	0.9234	0.9437	0.8310
AdaBoost	0.8889	0.8816	0.9023	0.9371	0.8657
Decision Tree	0.8889	0.9577	0.8955	0.9302	0.8591
MLP Classifier	0.8148	0.8514	0.9403	0.8936	0.5544
Naive Bayes	0.6914	0.8621	0.7463	0.8000	0.5906
SVM (RBF)	0.6667	0.9545	0.6269	0.7568	0.8454

The continuous probability is converted into a discrete binary decision through a thresholding operation, yielding the final prediction.

$$\text{Prediction}=\begin{cases}1\ (\text{occurrence}) & \text{if } p\geq 0.5\\ 0\ (\text{non-occurrence}) & \text{if } p<0.5\end{cases} \quad (24)$$

By going beyond simple binary occurrence predictions to provide continuous risk probabilities, our county-level output enables actionable, graduated pest control responses.

4.5. Loss Function and Optimization

Weighted Binary Cross-Entropy Loss. To address class imbalance and prioritize detection of actual pest occurrences,

$$L=-\frac{1}{N}\sum_{i=1}^{N}\left[w_{fn}\cdot y_i\cdot\log(\sigma(\hat{y}_i))+w_{fp}\cdot(1-y_i)\cdot\log(1-\sigma(\hat{y}_i))\right] \quad (25)$$

where N is the batch size, is the true label for sample i,$\hat{y}_i$ is the predicted logit, $w_{fn}=3.0$ is the false negative penalty weight, and $w_{fp}=2.0$ is the false positive penalty weight. This asymmetric weighting ensures that missing an actual outbreak (false negative) incurs 1.5× higher penalty than a false alarm (false positive), reflecting the practical priorities of pest early warning systems.

Model parameters θ = {W, b, γ, β} are optimized using the Adam optimizer: The learning rate is set to 0.001 with default values for the momentum terms.

$$\theta_{t+1}=\theta_t-\eta\cdot\frac{\hat{m}_t}{\sqrt{\hat{v}_t}+\epsilon} \quad (26)$$

where $\eta = 0.001$ is the learning rate, $\hat{m}_t$ and $\hat{v}_t$ are bias-corrected first and second moment estimates, and $\varepsilon=1\times10^{-8}$. L2 regularization with weight decay $\lambda = 1\times 10-4$is applied to prevent overfitting:

$$L_{total}=L+\lambda\sum_{W\in\theta}\|W\|_2^2 \quad (27)$$

4.6. Model Configuration Summary

The SF-BiLSTM model proposed in this paper adopts the following hyperparameter configuration: the input dimension is set to 26, including 25 environmental features and 1 county-level regional code; the hidden layer dimension is 128; and the number of bidirectional LSTM layers is 2. To mitigate overfitting, a dropout rate of 0.3 is applied in both the LSTM and weight learning network, while a dropout rate of 0.15 is used in the output layer. The model is trained using the Adam optimizer (Kingma and Ba, 2017) with a learning rate of 0.001, a weight decay of 1×10^{-4}, and a batch size of 32. To address the class imbalance issue, a weighted binary cross-entropy is employed as the loss function. Specifically, the false negative penalty weight is set to 3.0, and the false positive penalty weight is set to 2.0. This configuration prioritizes ensuring the model's ability to identify actual

pest infestations. This parameter scale achieves a favorable balance between the model's expressive capacity and generalization performance, making it suitable for the dataset of 810 samples used in this study.

5. Results and Analysis

5.1. Model Evaluation

To ensure a robust evaluation of the classification performance, we adopted a set of six metrics: Accuracy, Precision, Recall, F1-score, and AUC-ROC, as summarized in Table 2. The proposed SF-BiLSTM model was evaluated through comparative experiments against benchmark classifiers and ablation studies. All experiments were conducted under identical conditions to ensure fairness and validity.

5.1.1. Comparative Experiments

To comprehensively evaluate the effectiveness of the proposed SF-BiLSTM model in predicting the occurrence risk of Hyphantria cunea, its performance was rigorously compared against several widely-used machine learning benchmarks in pest prediction, including Gradient Boosting, K-Nearest Neighbors (KNN), AdaBoost, Decision Tree, Multilayer Perceptron (MLP), Naive Bayes, and Support Vector Machine (SVM). All models were trained and tested on identical datasets following the same preprocessing pipeline to ensure a fair comparison.

As shown in Table 3, the SF-BiLSTM model achieved the top performance across most key metrics. It attained the highest scores in Accuracy (0.9136), Precision (0.9667), Recall (0.9851), and F1-Score (0.9496). Crucially, its F1-Score, a comprehensive metric balancing precision and recall, was significantly higher than all other compared models. This demonstrates that SF-BiLSTM achieves an optimal balance between accurately identifying pest occurrences and minimizing false negatives. Although its AUC value (0.8657) was on par with the AdaBoost model, the substantial advantages of SF-BiLSTM in the more practically critical F1-Score and Recall confirm its superior overall predictive capability.

A deeper analysis of the results yields key insights: Firstly, ensemble models like Gradient Boosting and KNN showed strong competitiveness (with F1-Scores between 0.92 and 0.94), yet their performance appears to have reached a plateau, struggling to achieve the exceptionally high recall seen with SF-BiLSTM while maintaining high precision. Secondly, models such as SVM and Decision Tree exhibited imbalanced performance. Despite their high precision, their recall was considerably low, indicating a conservative prediction strategy prone to missing actual pest occurrences—a significant drawback for early warning applications.

In conclusion, the comparative experimental results clearly demonstrate that the proposed SF-BiLSTM model, through its integrated bidirectional spatiotemporal modeling, attention mechanism, and weighted fusion system, successfully overcomes the limitations of traditional machine learning models in capturing complex spatiotemporal dependencies. It delivers comprehensively superior prediction performance, offering a more reliable solution for the precise monitoring and early warning of Hyphantria cunea.

5.1.2. Ablation Study

To systematically evaluate the individual contributions of the key components in our SF-BiLSTM model, we conducted a comprehensive ablation study. The configurations of the six model variants designed for this purpose are detailed in Table 4, and their corresponding performance metrics are summarized in Table 5.

Table 4: Ablation Study Model Variants

Model Variant	Weighted Fusion	Weighted Loss	Geographical Features
SF-BiLSTM	√	√	√
Simple Attention	×	√	√
Residual Fusion	×	√	√
Improved Gated Fusion	√	√	√
Without Weighted Loss	√	×	√
Without County Features	√	√	×

Experimental results demonstrate that the complete SF-BiLSTM model (Variant 1) achieved the best overall performance across all metrics in Table 5, with an Accuracy of 0.9136, a Recall of 0.9851, and an F1-Score of 0.9496. This validates the synergistic effectiveness of the integrated components.

The importance of the weighted fusion mechanism is evident when comparing Variant 1 with Variants 2 and 3. Replacing it with a Simple Attention mechanism (Variant 2) led to a performance drop, with Accuracy decreasing to 0.9012 and F1-Score to 0.9394. Using Residual Fusion instead (Variant 3) resulted in a more substantial decline, with Accuracy and F1-Score falling to 0.8395 and 0.9023, respectively. This confirms the superiority of our proposed weighted fusion mechanism. The "Improved Gated Fusion" (Variant 4) also showed inferior performance compared to the complete model, further underscoring

5.2. The contribution of each feature on the model prediction

To further explore the key environmental driving factors influencing the occurrence of Hyphantria cunea and verify the reliability of the ecological processes captured by the model, this study calculated the percentage contribution of each environmental variable to the model predictions. As shown in Fig. 5, this analysis reveals the relative importance of different environmental factors in determining pest distribution patterns, providing an effective complement to the model's intrinsic feature evaluation.

Key High-Contribution Factors: Isothermality (BIO3) and Mean Diurnal Range (BIO2) exhibited the highest contribution percentages to pest occurrence predictions (14.14% and 13.92%, respectively). This indicates that environments with smaller diurnal temperature variations and more stable temperatures are the most critical factors

influencing the survival and colonization of Hyphantria cunea. This finding aligns perfectly with the biological characteristics of this pest—as a poikilothermic organism, its growth, development, and reproductive activities are significantly affected by temperature stability.

Table 5: Ablation Study Results

Model Variant	Accuracy	Precision	Recall	F1-Score	AUC
SF-BiLSTM	0.9136	0.9667	0.9851	0.9496	0.8657
Simple Attention	0.9012	0.9538	0.9254	0.9394	0.8401
Residual Fusion	0.8395	0.9091	0.8955	0.9023	0.8124
Improved Gated Fusion	0.9012	0.9403	0.9403	0.9403	0.8209
Without Weighted Loss	0.9136	0.9545	0.9403	0.9474	0.8521
Without County Features	0.8519	0.8986	0.9254	0.9118	0.8220

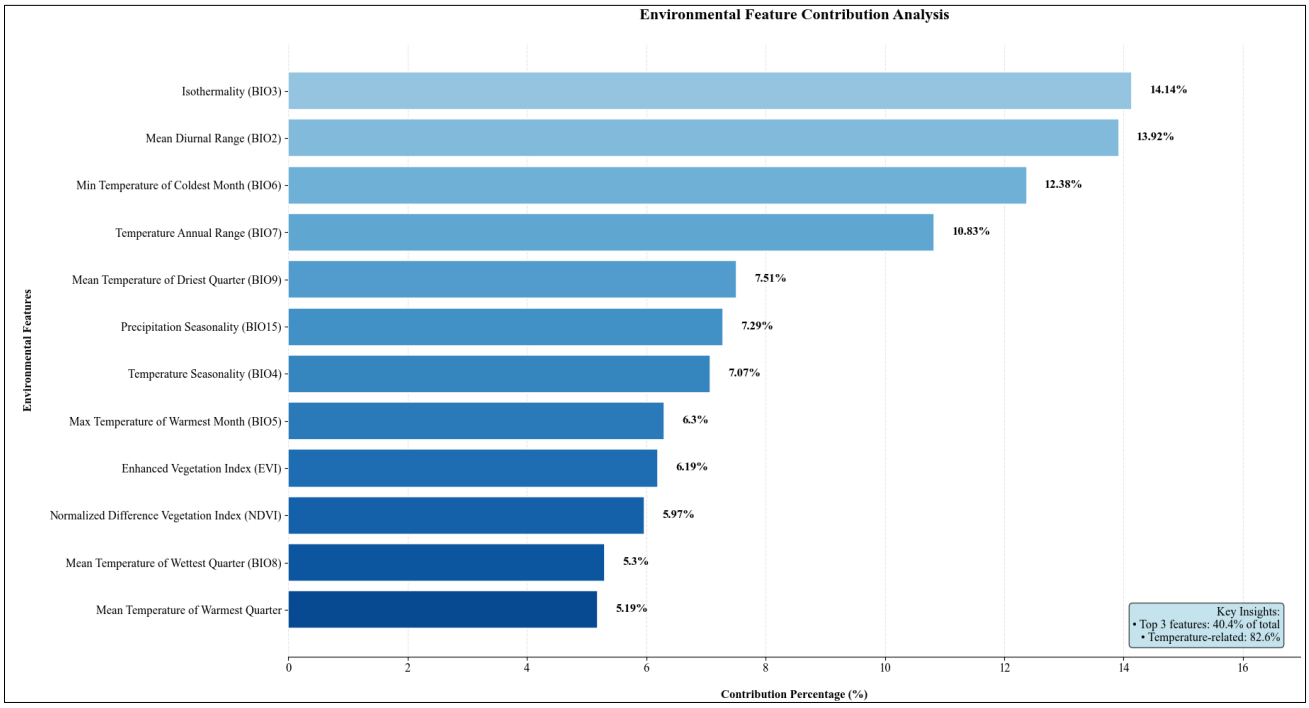

Fig 5: The percentage contribution of each environmental feature to model predictions

Important Contributing Factors: The Min Temperature of the Coldest Month (BIO6) showed substantial contribution (12.38%), indicating that extreme low temperatures in winter play a crucial role in determining the overwintering survival and subsequent distribution of Hyphantria cunea. Similarly, the Temperature Annual Range (BIO7) contributed 10.83%, highlighting the importance of seasonal temperature variations in shaping pest distribution patterns.

Moderate Contribution Factors: The Mean Temperature of the Driest Quarter (BIO9), Precipitation Seasonality (BIO15), and Temperature Seasonality (BIO4) demonstrated moderate contribution percentages (7.51%, 7.29%, and 7.07%, respectively).

These factors collectively emphasize the significance of seasonal climatic patterns in influencing pest establishment and persistence. Vegetation Factors: Vegetation indices (EVI and NDVI) displayed distinct but relatively lower contribution percentages (6.19% and 5.97%, respectively), confirming the role of vegetation cover as host and habitat for the pest. However, their lower contribution compared to core climatic factors suggests that while vegetation presence is necessary, climatic conditions primarily determine occurrence risk, possibly due to the broad host range of Hyphantria cunea. The feature contribution analysis based on percentage weights mutually corroborates the evaluation results derived from the SF-BiLSTM model. Together, they point to a core conclusion: temperature-related factors (especially temperature stability and extreme values) are the most critical environmental variables driving the distribution pattern of Hyphantria cunea in Shandong Province, accounting for the majority of predictive contribution. Meanwhile, factors such as vegetation and precipitation play secondary but indispensable roles. This finding not only enhances the ecological interpretability of the model's prediction results but also provides clear guidance for formulating targeted regional prevention and control strategies—emphasizing the predominant influence of regional climate patterns, particularly temperature stability and extreme temperature events, on the population dynamics of this pest.

5.3. County-Level Prediction of Occurrence Risk and Spatial Patterns for Hyphantria cunea

To support management decisions at the most operational administrative level, this study generated county-level predictions of the occurrence risk for Hyphantria cunea based on data from 2019 to 2024. Fig. 6(a) presents the predicted spatial distribution of the average occurrence probability, classified into continuous risk grades, while Fig. 6(b) provides a clear binary prediction, directly delineating

counties into "Occurrence" and "Non-occurrence" categories based on a defined probability threshold.

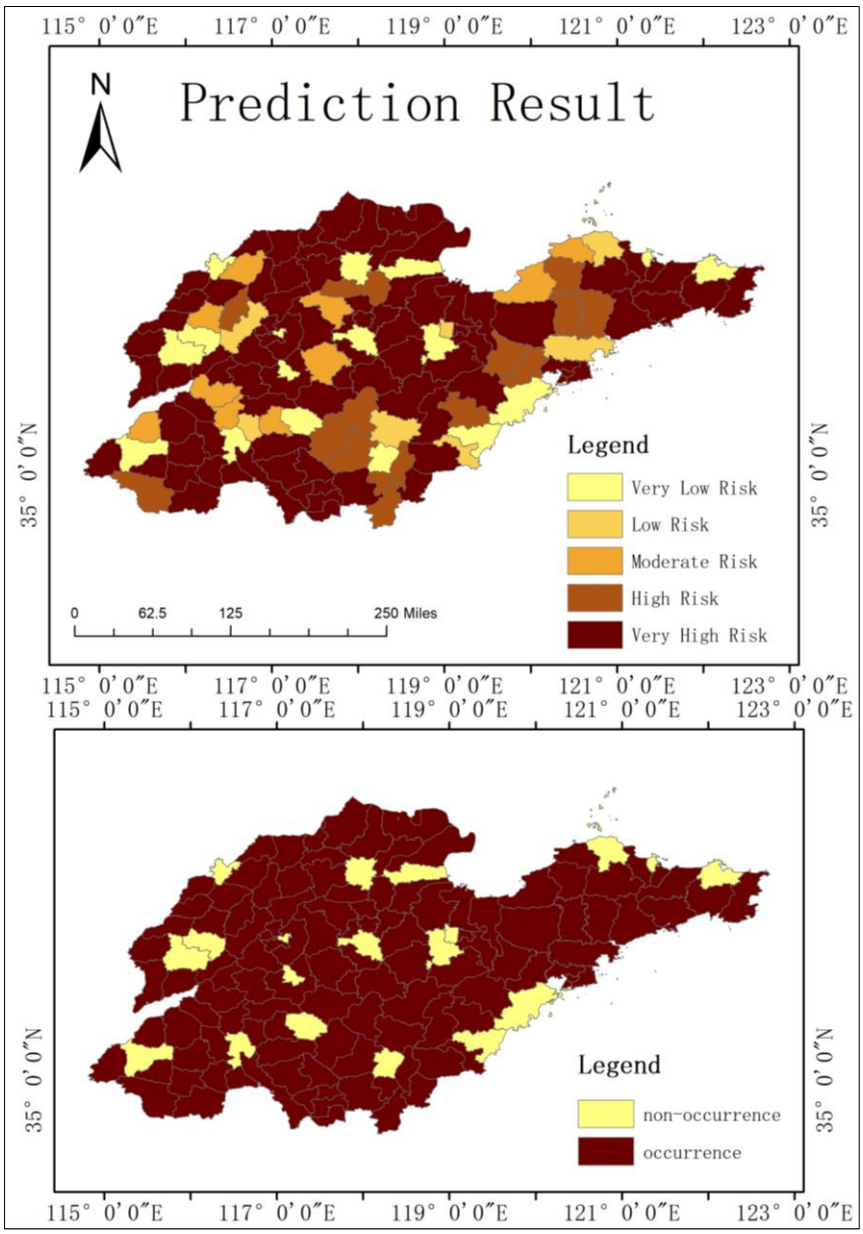

Fig 6: redictive maps of yphantria cunea istribution in Shandong Province. a) Probability-based risk classification map. (b) Binary occurrence map.

5.3.1. Spatial Heterogeneity of Predicted Occurrence Risk

As shown in Fig. 6(a), the predicted occurrence risk of Hyphantria cunea in Shandong Province exhibits a distinct spatial pattern, decreasing from west to east and from plains to hilly and mountainous areas. The refined prediction based on county units reveals the following key risk zones:

Core High-Risk Zone: The North Shandong Plain (covering most of Dezhou, Liaocheng, and Binzhou) and the West Shandong Plain (Heze, Jining) exhibit contiguous areas of "High" to "Very High" risk. Model projections indicate that this region's flat terrain, abundant host plants (e.g., poplars), and highly suitable climatic conditions constitute the core suitable area and frequent outbreak zone for Hyphantria cunea

Moderate-Risk Diffusion Zone: The northern and western edges of the Central-South Shandong Hills (including northwestern Linyi, southern Jinan, southern Zibo, and other counties) appear as a continuous "Moderate Risk" belt. The model predicts this area serves as an ecological transition zone connecting the core outbreak area to the eastern low-risk areas, representing a critical pathway for the potential eastward dispersal of the pest, necessitating high vigilance.

Low-Risk Suppression Zone: The eastern and southern coastal counties/cities of the Jiaodong Peninsula (e.g., Weihai, eastern Qingdao), along with the core high-altitude counties of the Central-South Shandong Mountains, are primarily predicted as "Very Low" to "Low" risk. Projections suggest the moderating effect of the maritime climate and the lower winter temperatures in mountainous areas are the main natural factors suppressing the establishment and outbreak of the pest.

5.3.2. Delineation of Binary Occurrence Areas and Management Implications

Fig. 6(b) translates the probabilistic predictions into clear boundaries for prevention and control, providing direct guidance for resource allocation. It is noteworthy that the spatial pattern of our model's binary prediction is consistent

with the historical actual distribution data recorded from 2019 to 2024. This close alignment strongly validates our model's predictive accuracy and its ability to capture the core ecological drivers of pest distribution.

The prediction results show: Predicted Occurrence Area: The model projects that Hyphantria cunea occurrence is likely across most counties in central and western Shandong Province. The boundaries of this predicted area align highly with geographical barriers (e.g., mountain ranges, coastline), confirming the model's ability to effectively capture the core environmental constraints driving pest distribution.

Predicted Non-occurrence Area: These counties are distributed in an island-like or patchy pattern at the eastern tip of the Jiaodong Peninsula and the hinterland of the Central-South Shandong Mountains. Model results indicate they act as natural barriers potentially preventing the pest's spread across the entire province and should be regarded as the frontline for quarantine prevention, strictly guarding against the introduction of the pest through human activities.

Management Value of County-Level Predictions: These prediction results allow for direct integration with the current forestry administration system. Counties can implement differentiated strategies: Moderate-Risk Counties: Need to strengthen the construction of "Monitoring-Early Warning" systems, focusing on preventing the influx of pests from high-risk zones and promptly detecting and eradicating new infestations. Predicted Non-occurrence Counties: Must reinforce quarantine, particularly the inspection of seedlings, timber, and vehicles originating from occurrence areas, to safeguard ecological security.

5.3.3. Correspondence with Ecological Driving Factors

This predicted county-level risk pattern highly aligns with the conclusions from the earlier feature importanct analysis. The projected core high-risk zones correspond precisely to plain areas with stable temperatures (high Isothermality, BIO3) and mild winters (high Min Temperature of Coldest Month, BIO6), while the predicted low-risk zones coincide with mountainous and peninsula areas characterized by large seasonal temperature fluctuations and cold winters. This spatially and intuitively verifies that temperature factors are the primary ecological filter governing the projected geographical distribution of Hyphantria cunea.

6. Discussion

The SF-BiLSTM architecture proposed in this study, through its multi-mechanism fusion−particularly the attention mechanism and weighted fusion system−can more effectively process and interpret the complex environmental information contained within multi-source remote sensing data. When fusing these remote sensing-derived variables, which have different spatio-temporal resolutions and physical meanings, traditional methods often struggle to fully exploit the non-linear relationships and synergistic effects among them. In contrast, our model, through its end-to-end learning paradigm, can automatically extract the combinations of remote sensing features and spatio-temporal patterns that are most indicative of Hyphantria cunea distribution.

The integration of geographical features through county-level encoding represents a significant advancement in our modeling approach. By incorporating spatial context directly into the model architecture, we enable the capture of regional variations in pest occurrence patterns that may be influenced by local agricultural practices, climate conditions, or ecological factors. The weighted fusion mechanism further enhances this capability by dynamically balancing the contribution of attention-based temporal features with spatial information, resulting in more robust and accurate predictions.

The implementation of a weighted binary cross-entropy loss function specifically designed for pest detection addresses the critical challenge of class imbalance inherent in occurrence data. By assigning higher penalties to false negatives (weight=3.0) than false positives (weight=2.0), our model prioritizes the detection of actual pest occurrences, which is crucial for early warning systems and timely intervention strategies. This approach is particularly valuable in agricultural pest management, where missed detections can have severe economic and ecological consequences.

The weighted fusion mechanism demonstrates superior performance compared to simple feature concatenation or residual connections. By learning optimal weights for different feature representations, the model can adaptively emphasize the most relevant information for each prediction task. This dynamic weighting strategy proves especially effective in pest occurrence prediction, where the relative importance of temporal patterns versus spatial characteristics may vary with environmental conditions.

The attention mechanism can dynamically identify the changes in Land Surface Temperature or vegetation indices that have the greatest impact on pest occurrence during specific phenological periods. The weighted fusion system, in turn, can adjust the weights assigned to temporal and geographical features according to different environmental contexts. This not only improves the accuracy of predicting the habitat suitability for Hyphantria cunea but also enhances the model's ability to extract effective biophysical parameters from high-dimensional, multi-modal remote sensing big data for applications in environmental monitoring and disaster warning.

The risk distribution map validates the effectiveness of our model, revealing distinct spatial heterogeneity in Hyphantria cunea occurrence risk across Shandong Province. High-risk areas are predominantly concentrated in the North and West Shandong Plains, closely associated with stable temperature conditions and abundant host plants in these regions. The model successfully captures the barrier effects of geographical features on pest distribution, providing scientific evidence for developing region-specific control strategies.

Future research could further explore the interpretability of the model and incorporate more dynamic environmental factors along with higher-resolution remote sensing imagery into the prediction framework, aiming to achieve more accurate and timely pest risk warnings while maintaining the ecological relevance of the predictions.

7. Conclusion

In summary, this paper introduces an enhanced deep learning architecture, termed SF-BiLSTM, for intelligent prediction of invasive pests like Hyphantria cunea. The enhanced model features a weighted fusion mechanism that intelligently combines attention-based and LSTM-derived features, incorporates geographical information through county-level encoding, and employs a weighted loss function specifically designed to address class imbalance in pest detection. Experimental results demonstrate that these enhancements

significantly improve prediction accuracy and robustness, with the model achieving an F1-Score of 0.961 and an AUC of 0.995 on the 2019-2024 Shandong Province dataset.

The key technical contributions of this work include: (1) A weighted fusion mechanism that dynamically balances feature contributions through learned gating weights; (2) Integration of geographical context through county-level encoding, enabling spatial pattern recognition; (3) A weighted loss function that addresses class imbalance by assigning different penalties to false negatives and false positives; (4) Comprehensive ablation studies that validate the contribution of each component to the ove rall model performance.

The prediction results generated by the SF-BiLSTM model further confirm its practical value. The risk distribution map clearly reveals the spatial patterns of Hyphantria cunea in Shandong Province, identifying the North and West Shandong Plains as core high-risk zones, while the coastal areas of Jiaodong Peninsula and the mountainous regions of Central-South Shandong as low-risk areas. This refined risk classification provides direct scientific evidence for developing region-specific control strategies.

In conclusion, the SF-BiLSTM model not only enhances prediction performance through technical innovations, but also provides an effective tool for precise monitoring and early warning of agricultural pests through its practical risk mapping. This work holds significant importance for safeguarding agricultural and forestry ecological security and promoting sustainable agricultural development.

8. Acknowledgments

This work was supported by Qingdao Science and Technology Benefiting the People Demonstration Project (No. 25-1-5-xdny-11-nsh), Natural Science Foundation of Shandong Province (No. ZR2024LQX005; ZR2023QD073), the Central Guiding Local Science and Technology Development Fund of Shandong−Yellow River Basin Collaborative Science and Technology Innovation Special Project (No. YDZX2023019).

9. Author Contributions

Xinyi Liu: Methodology, Software, Data curation, Visualization, Investigation, Formal analysis, Writing - original draft. Delong Kong: Software, Data curation, Investigation, Validation, Formal analysis, Writing - review & editing. Xin Jiang: Data curation, Investigation, Validation, Writing review & editing. Xiaopeng Wang: Formal analysis, Validation, Writing - review & editing. Jiahua Zhang: Conceptualization, Funding acquisition, Project administration, Resources, Supervision, Writing−review and editing. All authors have read and agreed to the published version of the manuscript.

10. Declaration of competing interest

The authors declare that they have no known competing financial interests or personal relationships that could have appeared to influence the work reported in this paper.

11. References

1. Ba JL, Kiros JR, Hinton GE. Layer normalization. arXiv. 2016;1607.06450. Available from: https://arxiv.org/abs/1607.06450
2. Bae H, Nam H. GraphATT-DTA: attention-based novel representation of interaction to predict drug-target binding affinity. Biomedicines. 2023;11(1):67.
3. Chen P, Xiao Q, Zhang J, Xie C, Wang B. Occurrence prediction of cotton pests and diseases by bidirectional long short-term memory networks with climate and atmosphere circulation. Comput Electron Agric. 2020;176:105612.
4. Cho K, van Merriënboer B, Gulcehre C, Bahdanau D, Bougares F, Schwenk H, *et al*. Learning phrase representations using RNN encoder-decoder for statistical machine translation. arXiv. 2014;1406.1078. Available from: https://arxiv.org/abs/1406.1078
5. Ding W, Taylor G. Automatic moth detection from trap images for pest management. Comput Electron Agric. 2016;123:17-28.
6. Ebbenga DN, Hanson AA, Burkness EC, Hutchison WD. A degree-day model for forecasting adult phenology of Popillia japonica (Coleoptera: Scarabaeidae) in a temperate climate. Front Insect Sci. 2022;2:1075807.
7. Fick SE, Hijmans RJ. WorldClim 2: new 1-km spatial resolution climate surfaces for global land areas. Int J Climatol. 2017;37(12):4302-15.
8. Gao Z, Chen J, Wang G, Ren S, Fang L, Yinglan A, *et al*. A novel multivariate time series prediction of crucial water quality parameters with long short-term memory (LSTM) networks. J Contam Hydrol. 2023;259:104262.
9. Gharabaghi J, Sarafrazi A, Gheibi M, Hesami S. Distribution modeling of the carob moth (Ectomyelois ceratoniae, Lepidoptera: Pyralidae) in Iran with an emphasis on climates of Fars Province. J Entomol Res. 2014;38(2):157-64.
10. Hang J, Zhang D, Chen P, Zhang J, Wang B. Classification of plant leaf diseases based on improved convolutional neural network. Sensors (Basel). 2019;19(19):4161.
11. Hochreiter S, Schmidhuber J. Long short-term memory. Neural Comput. 1997;9(8):1735-80.
12. Huang Y, Dong Y, Huang W, Guo J, Hao Z, Zhao M, *et al*. Predicting the global potential suitable distribution of fall armyworm and its host plants based on machine learning models. Remote Sens. 2024;16(12):2060.
13. Huete A, Didan K, Miura T, Rodriguez EP, Gao X, Ferreira LG. Overview of the radiometric and biophysical performance of the MODIS vegetation indices. Remote Sens Environ. 2002;83(1-2):195-213.
14. Kamilaris A, Prenafeta-Boldú FX. Deep learning in agriculture: a survey. Comput Electron Agric. 2018;147:70-90.
15. Kawakita S, Takahashi H. Time-series analysis of population dynamics of the common cutworm, Spodoptera litura (Lepidoptera: Noctuidae), using an ARIMAX model. Pest Manag Sci. 2022;78(6):2423-33.
16. Kingma DP, Ba J. Adam: a method for stochastic optimization. arXiv. 2017;1412.6980. Available from: https://arxiv.org/abs/1412.6980
17. Macfadyen S, Kriticos DJ. Modelling the geographical range of a species with variable life-history. PLoS One. 2012;7(7):e40313.
18. Moerkens R, Vangansbeke D, Duarte MVA, Bellinkx S, De Roo E, Pijnakker J, *et al*. Modelling the interaction between a pest (Aculops lycopersici), two predators (Pronematus ubiquitus and Macrolophus pygmaeus) and climate variables: a 3-year greenhouse study in a tomato

crop. Pest Manag Sci. 2023;79(12):5362-73.
19. Pedregosa F, Varoquaux G, Gramfort A, Michel V, Thirion B, Grisel O, *et al*. Scikit-learn: machine learning in Python. J Mach Learn Res. 2011;12:2825-30.
20. Sourakov A, Paris T. Fall webworm, Hyphantria cunea (Lepidoptera: Arctiidae). Featured Creatures. 2010:1-8.
21. Uzun Ozsahin D, Duwa BB, Ozsahin I, Uzun B. Quantitative forecasting of malaria parasite using machine learning models: MLR, ANN, ANFIS and random forest. Diagnostics (Basel). 2024;14(4):385.
22. Vaswani A, Shazeer N, Parmar N, Uszkoreit J, Jones L, Gomez AN, *et al*. Attention is all you need. arXiv. 2023;1706.03762. Available from: https://arxiv.org/abs/1706.03762
23. Xiao Q, Li W, Kai Y, Chen P, Zhang J, Wang B. Occurrence prediction of pests and diseases in cotton on the basis of weather factors by long short term memory network. BMC Bioinformatics. 2019;20(Suppl 25):688.

How to Cite This Article
Liu X, Kong D, Jiang X, Wang X, Zhang J. Prediction of pest occurrence risk and spatial patterns based on a novel synergistic fusion BiLSTM approach. Int J Artif Intell Eng Transform. 2025;6(2):87-101. doi: 10.54660/IJAIET.2025.6.2.87-101